

# Can reliable torsion elastic constants be determined from FPA data on 24 and 27 base-pair DNAs?

Bryant S. Fujimoto, J. Michael Schurr\*

Department of Chemistry, Box 351700, University of Washington, Seattle, WA 98195-1700, United States

Received 19 December 2004; received in revised form 1 February 2005; accepted 1 February 2005

Available online 19 February 2005

## Abstract

Torsion elastic constants obtained from fluorescence polarization anisotropy (FPA) measurements on fifty-three 24 and 27 base-pair (bp) DNAs were recently reported [1,2] [F. Pedone, F. Mazzei, D. Santoni, Sequence-dependent DNA torsional rigidity: a tetranucleotide code, *Biophys. Chem.* 112 (2004) 77–88; F. Pedone, F. Mazzei, M. Matzeu, F. Barone, Torsional constant of 27-mer DNA oligomers of different sequences, *Biophys. Chem.* 94 (2001) 175–184]. The problem of extracting reliable torsion elastic constants ( $\alpha$ ) from FPA measurements on such short DNAs is examined in detail. The difficulty is illustrated by two (fictitious) 24 bp DNAs with ~5-fold different torsion elastic constants and 10% different initial anisotropies ( $r_0$ ), which exhibit practically indistinguishable anisotropy decays for all  $t > 1$  ns. FPA data were simulated for 24 bp DNAs with different input values of  $\alpha$  and  $r_0$  in the presence and absence of Poisson noise, and were fitted using different choices of the adjustable and fixed parameters. Experimental data for a 24 bp DNA were fitted in a similar manner. For either the simulated or experimental FPA data, it was *not* possible to determine *both* the initial anisotropy,  $r_0$ , and the torsion elastic constant,  $\alpha$ , in a *reliable* (i.e. statistically significant) manner *in the presence of Poisson noise*. When  $r_0$  is *assumed* to be fixed at any particular value in the fitting protocol, a unique best-fit value of  $\alpha$  is obtained, but that best-fit  $\alpha$  is extremely sensitive to small deviations of the assumed fixed value of  $r_0$  away from the input  $r_0$ -value of the simulated data. Pedone et al. fitted their FPA data by assuming that  $r_0=0.360$ , and adjusting  $\alpha$ , the hydrodynamic radius ( $R_H$ ), and effective length ( $L$ ). In fact, the reported best-fit values of  $R_H$  and  $L$  lay significantly outside their expected ranges. When this same fitting protocol is applied to simulated data for 27 bp DNAs, better overall agreement with the reported experimental values ( $\alpha$ ,  $R_H$ , and  $L$ ) is obtained for a model, wherein all DNAs have the *same* typical input  $\alpha=5.9 \times 10^{-12}$  dyn cm,  $R_H=10.0$  Å, and  $L=27$  (3.4)+2.7=94.5 Å, but a 1.00- to 1.13-fold *range* of  $r_0$ -values, than for the model of Pedone et al., wherein all DNAs have the *same* input  $r_0=0.360$ ,  $R_H=10.0$  Å, and  $L=94.5$  Å, but a ~3-fold *range* of  $\alpha$ -values. It is concluded that, in the absence of reliable *independent* estimates of  $r_0$  for every DNA, the  $\alpha$ -values reported for 24 and 27 bp DNAs cannot be regarded as experimentally justified. The reliability of the torsion elastic constants reported for the 136 distinct tetranucleotide steps, which are inferred from the values reported for the fifty-three 24 and 27 bp DNAs, is also briefly discussed.

© 2005 Elsevier B.V. All rights reserved.

**Keywords:** Torsion elastic constant; FPA; DNA

## 1. Introduction

Recently torsion elastic constants were reported for 43 different duplex DNAs, each of which contained only 24 bp [1]. Those were combined with ten additional

values reported previously for 27 bp oligomers [2] to create a data set containing 53 torsion elastic constants. In earlier studies, the same group of Pedone, Barone, Mazzei and coworkers also reported torsion elastic constants for other 27 bp DNA, RNA, and DNA–RNA hybrid duplexes and also for a 30 bp DNA containing a lesion [3–6]. Prior investigations of duplexes containing  $\leq 36$  bp by other groups were unable to obtain reliable estimates of the torsion elastic

\* Corresponding author. Tel.: +1 206 543 6681; fax: +1 206 685 8665.

E-mail address: [schurr@chem.washington.edu](mailto:schurr@chem.washington.edu) (J.M. Schurr).

constants, and *no* values were reported [7–10]. Even for longer duplexes in the range of 43–50 bp, where the torsion modes relax a much larger fraction of the total anisotropy on a considerably longer and more accessible time-scale, the extraction of reliable values of the torsion elastic constant was marginal, so values were not always reported, and the *relative* statistical errors (standard deviation/average) in the few reported values were substantial (15–43%) [7,9–14]. In many studies of duplex oligonucleotides, investigators have elected to fix the torsion elastic constant at a typical value, or at each of several values spanning a 2- or 3-fold range, in order to extract some other desired quantity, such as the effective hydrodynamic cylinder radius, with greater precision [7,9–14].

In references [1–14], the hydrodynamic properties and in some cases also the torsion elastic constant were assessed by measuring the temporal decay of the fluorescence polarization anisotropy (FPA) of intercalated ethidium in short DNA duplexes. In our laboratory these measurements were performed by time-correlated single-photon counting using an apparatus with an instrumental width (full width at half maximum (FWHM))  $\lesssim 80$  ps, which defines its effective time-resolution. In certain other laboratories, including that of Pedone et al., the FPA measurements were performed in the frequency domain using a series of modulation frequencies up to 40 MHz for the intensity of the exciting light [1,2,7–9], which limits the effective time resolution to 7–8 ns. Their frequency domain instrument is similar to that employed by Chirico and coworkers [10,13,14], and has considerably lower time resolution than typical time-correlated single-photon counting instruments like that in our laboratory [7,8,11,12,15]. There arises the question of how Pedone and coworkers managed to extract torsion elastic constants from such short DNAs. The principal difference between the studies of Pedone and coworkers [1–6] and those of other workers [7–15] is a *different choice of assumed fixed parameters* in fitting the data.

The number of *potentially* adjustable parameters in the theory, which is detailed in Appendix A, is much too large to enable determination of all of them for any given DNA, especially a DNA with  $N \leq 36$  bp. These parameters are: (1) the initial anisotropy  $r_0 = (0.4)ARF$ , where ARF is the amplitude reduction factor ( $0 \leq ARF \leq 1.0$ ) due to rapid ( $\sim 50$  ps) isotropic wobble of the dye in its binding site [15,16]; (2) the torsion elastic constant ( $\alpha$ ), which governs both the dynamics of twisting deformations and also the anisotropy amplitude carried by the uniform azimuthal spinning mode [15]; (3) the hydrodynamic radius ( $R_H$ ), to which the friction coefficient ( $\gamma \sim R_H^2$ ) and diffusion coefficient ( $D_{||}$ ) for the azimuthal rotation are very sensitive, and to which the diffusion coefficient for end-over-end tumbling ( $D_{\perp}$ ) is much less sensitive [7,8,15], especially for long DNAs; (4) the dynamic bending elastic constant ( $\kappa_d$ ) (or equivalently the dynamic persistence length,  $P_d = h\kappa_d/kT$ , where  $h$  is the

rise per base-pair, and  $k$  is Boltzman's constant), which governs both the dynamics of bending deformations and the anisotropy amplitude carried by the uniform tumbling mode; (5) the contour length of a DNA containing  $N$  base-pairs and a single intercalated ethidium,  $L = Nh + 2.7 \text{ \AA}$ , where  $2.7 \text{ \AA}$  is the rise per intercalated ethidium; and (6) the equilibrium persistence length, which governs the root-mean-squared curvature and average end-to-end distance, to which  $D_{\perp}$  is sensitive.

In deciding which parameters to fix and which to adjust, some general criteria apply. Normally, a parameter should be fixed only when (a) it is known to the required level of precision from *independent* experiments or theory; (b) it is *not* expected to vary with certain sample properties, such as DNA sequence, length, or extent of dimerization; (c) the quantity of interest, in this case the torsion elastic constant, is *insensitive* to small errors or changes in value of the fixed parameter, and (d) other adjustable parameters, such as  $R_H$  and  $L$ , or  $D_{\perp}$ , which are reasonably well-known, and are not expected to vary significantly from one 24 bp sequence to the next (in the absence of substantial intrinsic curvature), should *not* be found well outside their known ranges and should *not* be found to vary significantly among the different samples, when the chosen parameter is fixed. Pedone and coworkers have elected to fix the *initial anisotropy* at  $r_0 = 0.360$  (or equivalently  $ARF = 0.90$ ), independent of DNA sequence. It will be shown that this choice satisfies none of the criteria (a)–(d) above, and leads to a very large *apparent* variation of the torsion elastic constant with DNA sequence for 24 and 27 bp duplexes, as well as values of  $R_H$  and either  $h$  (or  $L$ ) for 27 bp duplexes that lie outside expected limits, as well as unexpectedly large variations of those same quantities among the different DNAs.

The objectives of the present study are (1) to show that two 24 bp DNAs with a  $\sim 5$ -fold ratio of torsion elastic constants and a 10% difference in  $r_0$  can exhibit anisotropy decays that are practically indistinguishable for all times,  $t > 1$  ns; (2) to show that  $\alpha$  and  $r_0$  *cannot* be both be determined from FPA data for a 24 or 27 bp DNA using instruments like that of Pedone et al. or that in our laboratory; (3) to note that for much longer DNAs, where  $\alpha$  and  $r_0$  *can* be simultaneously determined, the best-fit  $r_0$  does *not* always exhibit the same value, 0.360, but instead varies over a range from 0.31 to 0.38, and is sensitive to Poisson noise and other variations in the experimental data; (4) to show that a rather small error in the assumed fixed value of  $r_0$  can cause an extremely large error in the best-fit value of  $\alpha$ ; (5) to note that the values of  $R_H$  and  $L$  reported by Pedone et al. [2] for ten 27 bp duplexes differ from their expected values, and also among each other, by more than would be expected; and (6) to show that the 4.4-fold span of  $\alpha$ -values reported by Pedone et al. can be obtained by fitting FPA data that are simulated using a *single* value of  $\alpha$  and modestly different  $r_0$  values within the previously observed range of such values. The likelihood of validity of the 53

values reported by Pedone et al. [1] is discussed in detail. We also address briefly the reported determination of the effective torsion elastic constants of 136 tetranucleotide steps from these, or any other, set of 53 torsion elastic constants obtained for different DNAs that collectively contain all 136 tetranucleotide sequences.

## 2. Analysis of the problem

In the course of this discussion, we shall often refer to the relevant theory for the anisotropy function ( $r(t)$ ) [8,15], which is used to simulate FPA data and also to fit both simulated and experimental data. That theory, which was employed in one way or another in references [1–16], is presented in Appendix A, where its various parameters are also defined.

For a 24 bp DNA with an intercalated ethidium, the relaxation time of the longest torsion normal mode,  $\tau_2$ , is reckoned from Eq. (A10) in Appendix A using  $N+1=25$ , a typical torsion elastic constant,  $\alpha=5.9\times 10^{-12}$  dyn cm, a typical hydrodynamic radius  $R_H=10.0$  Å, a contour length,  $L=N\cdot(3.4)+2.7=84.3$  Å, and the fixed parameters in Table 1, which yields the friction factor for azimuthal rotation,  $\gamma=4.70\times 10^{-23}$  dyn cm s, and  $\tau_2=0.50$  ns. Similarly, the longest bending time ( $T_1$ ) is reckoned from Eq. (A17) in Appendix A, using the same fixed parameters in Table 1, including,  $P_d=1800$  Å cm for the dynamic persistence length, which yields  $T_1=0.14$  ns. (The latest studies indicate that  $P_d$  lies in the range 1800 (–200, +400) Å [17–19].) These times are much too short to be resolved by a frequency domain instrument that reaches only to  $\nu=40$  MHz, which can only “fully” resolve exponential decays with relaxation times  $\tau\geq 2/(2\pi\nu)\sim 8$  ns. Such an instrument can resolve only the *uniform mode decays* of the twisting and tumbling correlation functions that are indicated in Eqs. (A13) and (A19). For the same 24 bp DNA in aqueous buffer at 293 K,  $D_{||}$  and  $D_{\perp}$  are reckoned from Eqs. (A1) and (A3) [20], which yield  $D_{\perp}=6.493\times 10^6$  s $^{-1}$  and  $D_{||}=3.446\times 10^7$  s $^{-1}$ . The time constants for the  $n=2$ , 1, and 0 terms in Eq. (A6) are, respectively,  $(4D_{||}+2D_{\perp})^{-1}=6.6$  ns,  $(D_{||}+5D_{\perp})^{-1}=14.9$  ns, and  $(6D_{\perp})^{-1}=25.7$  ns, all of which should be (nearly) satisfactorily resolved by the frequency domain instrument. An essential point is that any information regarding the torsion elastic constant comes *not* from resolving the time course of the torsional deformation modes, but only from the *reduced amplitude*,  $B_n(\infty)$ , carried by the uniform spinning modes in the  $n=2$  and  $n=1$  terms in Eqs. (A6) and (A13). Unfortunately, these amplitude reductions due the (relaxed) twisting deforma-

tions cannot be reliably distinguished from the amplitude reduction due to dye wobble (i.e.  $ARF=r_0/0.4$ ) for such short DNAs, as will be seen. The situation is fundamentally different for longer DNAs with  $N\geq 50$  bp, where the temporal decay of the torsion modes is at least partially resolved, and the torsion elastic constant in favorable cases can be separated from ARF or  $r_0$ , *although its precision is low for DNAs as short as 50 bp* [10,13,14]. For a 43 bp DNA the relative error ( $\pm 43\%$ ) was *unacceptably large* [11].

In our laboratory, the best-fit value of  $r_0$  for a given sample of long DNA with  $N\geq 181$  bp typically varies from one data set to the next, which indicates that it is sensitive to Poisson noise. Moreover, after averaging over many data sets, the best-fit  $r_0$ -values for different long DNA samples are not always 0.36, but span the range, 0.31 to 0.38. The average best-fit  $r_0$ -values for short duplexes with 12–36 bp exhibit a similar range, 0.33–0.38, when  $\alpha$  is assumed to be fixed at the same (typical) value,  $5.9\times 10^{-12}$  dyn cm, for every DNA examined, and higher values in the range  $r_0=0.365$  to 0.380 are relatively more common (60%) than in the case of long DNAs (unpublished data). A number of experimental factors appear to contribute to small systematic variations in  $r_0$ , such as (i) sample-to-sample variations in the Rayleigh scattered light or any short-lived fluorescence from the filter, a very small percentage of which could reach the detector; (ii) variations in the ratio of non-intercalated to intercalated ethidium coupled with uncertainty regarding how much of the non-intercalated dye is free and how much is *outside* bound to the DNA in some unknown orientation [15]; (iii) temporal fluctuations in laser power or photomultiplier gain; (iv) temporal shifts of the instrument function; or (v) polarization artifacts arising from depolarization in the polarizers and/or different detection efficiencies for the parallel and perpendicular polarization configurations; and (vi) small amounts of unsuspected dimerization, which can occur for 12 bp duplexes at concentrations  $\geq 15$  mg/mL. The point is that the best-fit value of  $r_0$  is by no means always 0.360, and is sensitive to Poisson noise, as well as to small systematic experimental errors and inaccurate fitting functions.

Using a frequency domain instrument similar to that of Pedone and coworkers, Collini et al. obtained  $r_0=0.34$  to 0.345 for a 50 bp straight duplex, and  $r_0=0.325$  to 0.335 for a 50 bp bent duplex [13], when both  $r_0$  and  $\alpha$  were adjusted, and Chirico et al. found best-fit values,  $r_0=0.37$  to 0.39 for straight and intrinsically curved DNAs containing 31–111 bp, when the torsion elastic constant was fixed at  $8\times 10^{-12}$  dyn cm [10]. In short, there is no evidence to suggest that  $r_0$  is always 0.36 or any other single value. Nor is there any theoretical reason to expect that  $r_0$  should be the same for every sequence.

Ethidium binds to duplex DNAs with  $N\geq 7$  bp in a nearly random fashion, apart from neighbor exclusion, with a binding constant that is largely independent of DNA composition [21–32]. The torsion elastic constant is also

Table 1  
Common input parameters

$T$ (K)	$\varepsilon_0$ (°)	$\eta$ (P)	$P_d$ (Å)
293	70.5	0.001002	1800

largely independent of base composition [15,33]. Hence, some modest variation of  $r_0$  (or ARF) with sequence is *a priori* just as likely as some variation of the torsion elastic constant with sequence. The assumption that  $r_0=0.36$  for every measurement on every DNA sample fails to satisfy criteria (a) and (b) of the previous section for choice of adjustable parameter.

### 2.1. Indistinguishability of $r(t)$ curves with very different $\alpha$

Fig. 1 presents the theoretical anisotropy function,  $r(t)$  vs.  $t$ , for three rather different pairs of  $r_0$  and  $\alpha$  values, but identical values of the standard parameters in Table 1. The similarity of these curves is so striking that it suffices to discuss just the two curves with the greatest differences in  $r_0$  and  $\alpha$ . The  $r(t)$  curves for  $r_0=0.335$ ,  $\alpha=11.96\times 10^{-12}$  and for  $r_0=0.37$ ,  $\alpha=2.41\times 10^{-12}$  (Table 2), lie so close to one another, especially for  $t>1$  ns, that it would be practically impossible to distinguish between them in the presence of any realistic level of noise. This demonstrates that a very large ( $\sim 5$ -fold) reduction in  $\alpha$  can be almost completely compensated by a  $\sim 10\%$  increase in  $r_0$  to obtain essentially the same anisotropy decay curve. Conversely, a very large ( $\sim 5$ -fold) variation in  $\alpha$  is required to compensate a rather small ( $\sim 10\%$ ) change in  $r_0$ . Thus, fixing  $r_0$  at an even slightly erroneous value would introduce very large errors into the best-fit value of  $\alpha$ .

The corresponding frequency domain spectra for the modulation ratios and phase differences of the three  $r(t)$  curves in Fig. 2 were computed from the theoretical intensities in the absence of noise,  $I_{\parallel}(t)=2(t)(1+2r(t))/3$  and  $I_{\perp}(t)=S(t)(1-r(t))/3$ , where  $S(t)=S_0\exp[-t/\tau_E]$ , and  $\tau_E=22\times 10^{-9}$  s is the lifetime of intercalated ethidium. These computations followed the protocol of Chirico and coworkers [10,13,14]. Specifically, a 0.2 ns sampling time was employed and a fast Fourier transform of 4096 data points was performed for  $I_{\parallel}(t)$  and  $I_{\perp}(t)$  in each case, and the demodulation ratios and phase shifts were calculated at

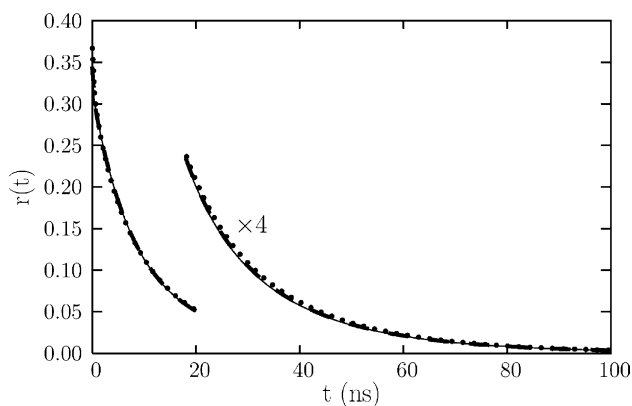


Fig. 1. Calculated noise-free  $r(t)$  vs.  $t$  for the three sets of parameters in Table 1. The thin line comes from set 1, the dashed line from set 2, and the dotted line from set 3. The instrumental width is assumed to vanish, corresponding to a delta function exciting pulse and an instantaneous response of the detection electronics.

Table 2

Standard input parameters for the  $r(t)$  curves in Fig. 1

Parameter set	$r_0$	$\alpha$ (dyn cm)	$R_H$ (Å)	$L$ (Å)
1	0.335	$11.96\times 10^{-12}$	10.04	83.52
2	0.345	5.86	10.04	83.52
3	0.370	2.41	10.04	83.52

each frequency according to the equations in Refs. [13,14]. The resulting noise-free frequency-domain spectra in Fig. 2 are virtually indistinguishable except for the phase differences above 30 MHz, where a very small difference is visible between the curve with  $r_0=0.335$ ,  $\alpha=11.96\times 10^{-12}$  dyn cm and that with  $r_0=0.37$ ,  $\alpha=2.41\times 10^{-12}$  dyn cm. The largest difference between these two  $\Delta\phi$  curves,  $0.4^\circ$ , occurs at 40 MHz. At the next lowest of the 20 frequencies sampled, namely 34.2 MHz, the difference is approximately  $0.2^\circ$ , and at all 18 lower sampled frequencies the difference between the two curves is considerably less than  $0.2^\circ$ . Pedone et al. state that the statistical “error” of a phase measurement ( $\phi_{\parallel}$  or  $\phi_{\perp}$ ) is  $0.2^\circ$ . Since two such measurements are combined to obtain the phase difference ( $\Delta\phi=\phi_{\perp}-\phi_{\parallel}$ ), the statistical error in that quantity would be  $0.28^\circ\approx 0.3^\circ$ . However, that value may be overly optimistic for the highest frequencies. Although Pedone et al. report no  $\Delta\phi$  vs. frequency data [1,2], such data were published in earlier communications from the same laboratory [3,4]. From the roughness of the consecutive data at the four highest frequencies it would appear that those errors

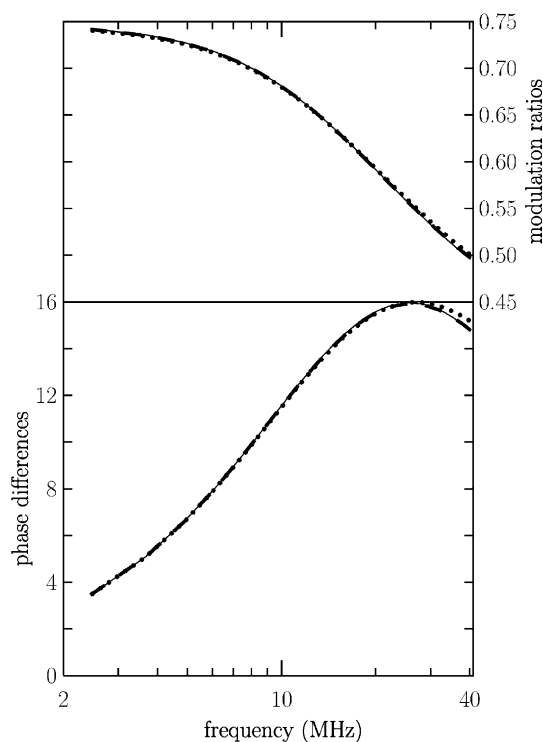


Fig. 2. Simulated noise-free modulation ratio and phase difference vs. frequency for the three sets of parameters in Table 2. The thin line comes from set 1, the dashed line from set 2, and the dotted line from set 3. The electronic detection response is assumed to be instantaneous.



in  $\Delta\phi$  are closer to  $0.4\text{--}0.5^\circ$ . The same conclusion is reached by examining the  $\Delta\phi$  vs. frequency curves reported by Chirico and coworkers, who employed a similar instrument [10,13,14]. The difference between the two noise-free theoretical  $\Delta\phi$  curves in Fig. 2 is either comparable to or less than the experimental error at 40 MHz, and is considerably less than the experimental error at all lower sampled frequencies. *In the presence of realistic noise*, these two curves could not be distinguished at any useful confidence level (or significant difference in  $\chi_r^2$ , defined below) by the instrument and protocol employed. This will be shown explicitly in the next section.

## 2.2. Inability of least-squares fitting to retrieve $\alpha$ and $r_0$ in the presence of Poisson noise

Is it possible to reliably determine the correct value of  $\alpha$  by fitting simulated FPA data containing Poisson noise with different assumed fixed values of  $r_0$ , and comparing the resulting  $\chi_r^2$ -values to determine the best choice of  $r_0$  and its corresponding best-fit value of  $\alpha$ ? In order to address this question, FPA data were simulated for  $r_0=0.360$  and 17 different input  $\alpha$ -values spanning the interval,  $(1.5 \text{ to } 9.0) \times 10^{-12}$  dyn cm, in steps of about  $0.5 \times 10^{-12}$  dyn cm, while holding constant  $R_H=10.0$  Å,  $L=84.3$  Å, and the standard parameters in Table 1. The intensities of fluorescence with polarizations parallel and perpendicular to that of the exciting pulse are given by [15]

$$i_{\parallel}(t) = (1/3) \int_0^t dt' e(t') S_0 \exp[-(t-t')/\tau_E] \cdot (1 + 2r(t-t')) \quad (1)$$

$$i_{\perp}(t) = (1/3) \int_0^t dt' e(t') dt' e(t') S_0 \exp[-(t-t')/\tau_E] \cdot (1 - r(t-t')) \quad (2)$$

wherein  $e(t)$  is the instrument function,  $S_0$  is the amplitude of the fluorescence intensity,  $\tau_E=22$  ns is the fluorescence lifetime of intercalated ethidium, and  $r(t)$  is calculated from Eq. (A6). The instrument function was taken to be an unnormalized Gaussian function centered at  $t_0=13.6$  ns in a total time interval that runs from 0 to 148 ns. The FWHM of the instrument function was taken to be 7 ns, to represent the time resolution of a 40 MHz frequency domain instrument. This can be seen by noting that the in- and out-of-phase frequency domain signals at a particular frequency are just the real and imaginary parts of the (one-sided) Fourier transform of either  $i_{\parallel}(t)$  or  $i_{\perp}(t)$ . Under the convolution theorem, such a Fourier transform is just the Fourier transform of  $e(t)$  times that of  $S_0 \exp[-t/\tau_E](1+2r(t-t'))$  or that of  $S_0 \exp[-t/\tau_E](1-r(t-t'))$ . The Fourier transform of the Gaussian,  $e(t)=(2\pi\sigma_t^2)^{-1/2} \exp[-(t-t_0)^2/2\sigma_t^2]$ , is  $E(\omega)=\exp[-\omega^2\sigma_t^2/2]$ , where  $\omega=2\pi\nu$ , so the contributions of frequencies above  $\nu=40$  MHz, where  $\omega\sigma_t \gtrsim 1.0$ , are very strongly attenuated. The height of the Gaussian was chosen

so that  $\int_0^{148 \times 10^{-9}} e(t) dt = 9.3 \times 10^4$  photon counts, and  $S_0$  was then chosen so that  $\int_0^{148 \times 10^{-9}} i_{\parallel}(t) dt = 3.3 \times 10^6$  counts and  $\int_0^{148 \times 10^{-9}} i_{\perp}(t) dt = 2.4 \times 10^6$  counts. The integrated numbers of counts in  $e(t)$ ,  $i_{\parallel}(t)$ , and  $i_{\perp}(t)$  are more than twice what we usually collect in a single data set before fitting. The time was divided into 0.16 ns intervals to perform the convolutions. The final synthetic  $i_{\parallel}(t)$  and  $i_{\perp}(t)$  values were obtained by adding the appropriate Poisson noise to each “channel,”  $i_{\parallel}(t)$  and  $i_{\perp}(t)$ , using the POIDEV function [34]. A different random number seed was used for each set of simulated FPA data. From  $i_{\parallel}(t)$  and  $i_{\perp}(t)$ , the simulated sum ( $s(t)$ ) and difference ( $d(t)$ ) functions were reckoned according to [15]

$$s(t) = i_{\parallel}(t) + 2i_{\perp}(t) = \int_0^t dt' e(t') S_0 \exp[-(t-t')/\tau_E] \quad (3)$$

$$d(t) = i_{\parallel}(t) - i_{\perp}(t) = \int_0^t dt' e(t') S_0 \exp[-(t-t')/\tau_E] r(t-t') \quad (4)$$

The anisotropy function used to fit  $d(t)$  is given by Eq. (A6) with  $r_0$  fixed at each of a series of values (0.33, 0.34, 0.35, 0.36, 0.37, 0.38) with adjustable  $\alpha$ ,  $R_H$ , and  $L$ , and with other parameters fixed at the standard values in Table 1. To simulate the FPA data,  $D_{\perp}$  was computed using Eq. (A1) in Appendix A with  $\zeta=1.017$ . However, in the fitting process for this example, no account was taken of any shortening of the effective length due to spontaneous curvature, which corresponds to the protocol employed by Pedone et al., wherein the adjusted  $L$  should be regarded as an *effective* contour length. The instrument function used in the fitting procedure to deconvolute the simulated data was the same Gaussian function used to calculate the simulated data, except that now Poisson noise was added to mimic the *experimental* instrument function. The fitting of Eqs. (3) and (4) to their respective synthetic data was carried out by a standard convolute and compare approach, implemented via the Marquardt algorithm [35], to minimize the reduced chi-squared ( $\chi_r^2$ ), as described previously [15]. ( $\chi_r^2 = (1/N) \sum_{j=1}^N (d(t_j)^{\text{th}} - d(t_j)^{\text{exp}})^2 / \sigma_{d_j}^2$ , where  $\sigma_{d_j}^2$  is the variance (due to Poisson noise) of the “experimental” measurement,  $N$  is the number of data channels, and the superscripts, “th” and “exp” denote theoretical and “experimental” values, respectively).

The questions addressed here are whether there exists a significant minimum in a plot of  $\chi_r^2$  vs. assumed fixed value of  $r_0$ , when the assumed fixed value of  $r_0$  exactly matches the input value,  $r_0=0.36$ , and whether the best-fit value of  $\alpha$  for that “correct” choice of fixed  $r_0=0.36$  also matches its input value.

Seventeen simulated data sets with different input  $\alpha$ -values, but the same input  $r_0=0.360$ , were fitted by using each of six different fixed values of  $r_0$ . For purposes of comparison,  $\chi_r^2$  values were reckoned to the second place to

the right of the decimal, which suffices for discrimination at the  $\sim 1\%$  level, well below the  $\sim 10\%$ -level required for statistical significance. In no case did a *unique* minimum in  $\chi_r^2$  occur at  $r_0=0.360$ , and in 4 of the 17 cases, the  $\chi_r^2$  value for the assumed fixed  $r_0=0.360$  exceeded the lowest  $\chi_r^2$  value(s) for other choice(s) of  $r_0$  by 0.01. Generally, there was no *significant* variation of  $\chi_r^2$  with the assumed fixed value of  $r_0$ , except for the choice  $r_0=0.33$ , where  $\chi_r^2$  values exceeding 1.1 were obtained for certain input  $\alpha$ -values, namely for  $\alpha=(5.5$  to  $9.0)\times 10^{-12}$  dyn cm, for which  $\chi_r^2$ -values from 1.12 to 1.26 were observed. In all of these cases, unphysically large best-fit values,  $\alpha \geq 2.1 \times 10^{-2}$  dyn cm, were obtained. In fact, when  $r_0=0.33$ , unphysically large values,  $\alpha \geq 1.4 \times 10^{-9}$  dyn cm, were obtained for *all* of the larger input  $\alpha$ -values,  $\alpha \geq 3.50 \times 10^{-12}$  dyn cm. Likewise, for the choice  $r_0=0.34$ , unphysically large best-fit values,  $\alpha \geq 1.1 \times 10^{-2}$  dyn cm, were also obtained for all of the larger input values,  $\alpha \geq 6.50 \times 10^{-12}$  dyn cm. However, in all of these latter cases,  $\chi_r^2 \leq 1.05$ . Unphysically large best-fit  $\alpha$ -values are always found for the larger input  $\alpha$ -values and smaller assumed fixed  $r_0$ -values, simply because the simulated  $r(t)$  curves with  $r_0=0.360$  and one of the larger input  $\alpha$ -values exhibit such high values that, when  $r_0$  is assumed to be fixed at too low a value in the fitting protocol, it is no longer possible to compensate by increasing  $\alpha$  within any reasonable bounds, so  $\alpha$  diverges.

Fig. 3 presents plots of  $\chi_r^2$  vs. assumed fixed  $r_0$  for fits to three simulated data sets, which were created using  $r_0=0.360$  and very different values of  $\alpha$ , specifically  $(1.7, 4.5$  and  $8.0)\times 10^{-12}$  dyn cm). These  $\chi_r^2$  are essentially flat over the entire range of assumed fixed  $r_0$ , except for the case where synthetic data were created using  $\alpha=8.0 \times 10^{-12}$  dyn cm and fitted using an assumed fixed  $r_0=0.330$ , for which  $\chi_r^2=1.26$ . That value lies significantly above the other  $\chi_r^2$ -values. Apart from this one point, there is no *statistical* basis for selecting any one value of  $r_0$  in the range 0.33 to 0.38 over any other. The best-fit values of  $\alpha$  are also plotted vs. assumed fixed value of  $r_0$  in the upper part of Fig. 3. When the assumed fixed value of  $r_0$  matches the input value, 0.360, the best-fit values of  $\alpha$  compare with their respective input values as follows:  $\alpha=(2.23$  vs.  $1.70)\times 10^{-12}$ ;  $\alpha=(4.17$  vs.  $4.50)\times 10^{-12}$ ;  $\alpha=(8.44$  vs.  $8.0)\times 10^{-12}$  dyn cm. The 31% error in best-fit  $\alpha$  for the case when input  $\alpha=1.70 \times 10^{-12}$  dyn cm, indicates that, even when  $r_0$  is fixed at the correct input value, 0.360, there are still too many parameters ( $\alpha$ ,  $R_H$ , and  $L$ ) that can be traded off against one another to produce fits of nearly equivalent  $\chi_r^2$  with significantly different values of the best-fit parameters. In that particular example, the best-fit  $L=89.75$  Å significantly exceeds the expected value 83.53 Å (obtained from fits to noise-free data), and the best-fit  $R_H=9.19$  Å lies significantly below the input  $R_H=10.0$  Å. For the other two cases,  $\alpha=(4.5, 8.0)\times 10^{-12}$  dyn cm, where closer agreement between the best-fit and input  $\alpha$ -values prevails, the best-fit  $L$ -values (82.08, 85.25 Å) and  $R_H$ -values (10.19, 9.91 Å) lie much closer to their expected values.

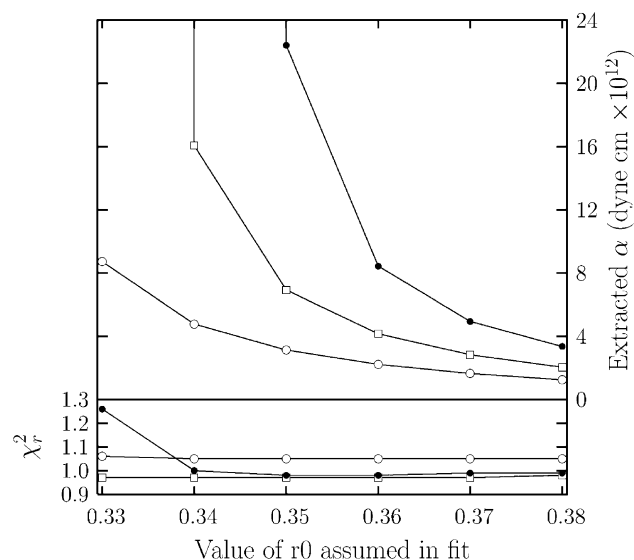


Fig. 3.  $\chi_r^0$  and best-fit  $\alpha$ -value from fits to three sets of simulated FPA data (with Poisson noise) vs.  $r_0$ -value assumed in the fit. The three sets of simulated data differ only in the value of  $\alpha$  used to create them.  $\circ$ :  $\alpha=1.7 \times 10^{-12}$  dyn cm;  $\square$ :  $\alpha=4.5 \times 10^{-12}$  dyn cm;  $\bullet$ :  $\alpha=8.0 \times 10^{-12}$  dyn cm. The other parameters used to create the simulated data were  $r_0=0.36$ ,  $R_H=10.0$  Å,  $L=84.3$  Å,  $D_{\perp}=6.493 \times 10^6$  s $^{-1}$ ,  $P_d=1800$  Å,  $\epsilon=70.5^\circ$ ,  $T=293$  K, and  $\eta=0.01002$  P. The instrument function was a Gaussian with 7 ns width, and Poisson noise was added to the calculated  $i_{\parallel}(t)$  and  $i_{\perp}(t)$ . The adjustable parameters in each fit are  $\alpha$ ,  $R_H$ , and  $L$ , while all other parameters except  $r_0$  are held fixed at their input values. Three of the best-fit values of  $\alpha$  are too large to be plotted on this figure. For the simulated data with  $\alpha=4.5 \times 10^{-12}$ , the best-fit  $\alpha$  for assumed  $r_0=0.33$  is  $1.2 \times 10^{-3}$  dyn cm. For the data simulated with  $\alpha=8.0 \times 10^{-12}$ , the best-fit  $\alpha$ -values are  $1.3 \times 10^{-3}$  dyn cm for assumed  $r_0=0.33$ , and  $1.1 \times 10^{-2}$  dyn cm for assumed  $r_0=0.34$ .

It is evident from Fig. 3 that errors in the best-fit  $\alpha$ -values can be extremely large, when the assumed fixed value of  $r_0$  differs from the input  $r_0$ -value by as little as 0.01, especially when the input  $\alpha$ -value exceeds  $5.5 \times 10^{-12}$  dyn cm. As the assumed fixed  $r_0$ -value varies from  $r_0=0.38$  to 0.33, the best-fit  $\alpha$ -value ranges from (i)  $(1.25$  to  $8.72)\times 10^{-12}$  dyn cm, a span of 7-fold, for input,  $\alpha=1.70 \times 10^{-12}$  dyn cm; (ii)  $(2.05 \times 10^{-12}$  to  $1.2 \times 10^{-3})$  dyn cm, a span of  $5.9 \times 10^8$ -fold, for input  $\alpha=4.50 \times 10^{-12}$  dyn cm; and (iii)  $(3.36 \times 10^{-12}$  to  $1.3 \times 10^{+3})$  dyn cm, a span of  $3.9 \times 10^{14}$ -fold, for input  $\alpha=8.0 \times 10^{-12}$  dyn cm. Clearly, the best-fit  $\alpha$  is *inordinately sensitive* to relatively small ( $\pm 0.01$ ) variations in the assumed fixed value of  $r_0$ ! Thus adoption of  $r_0$  as an assumed fixed parameter in fitting the FPA data strongly violates criterion (c), as well as (a) and (b), of Introduction.

The explanation for the unphysically large best-fit  $\alpha$ -values was stated above. Suffice it to say here that the assumed fixed value of  $r_0$  must be known with exceptional precision, much better than  $\pm 0.01$ , in order to prevent extremely large errors in the best-fit  $\alpha$ -values, *when proper account is taken of dynamic bending*, as was done here.

Next, one might inquire whether fixing also the values of  $L$  and  $R_H$  at their expected values, in addition to fixing  $r_0$ , during the fitting of simulated data would enable a statistically significant minimum to be found in the plot of  $\chi_r^2$  vs.

assumed fixed  $r_0$ -value, and thereby allow a determination of both  $r_0$  and  $\alpha$  for a 24 bp DNA. Such fitting of the same simulated FPA data described above was performed with fixed  $L=84.3$  Å,  $R_H=10.0$  Å and  $D_{\perp}=6.493 \times 10^6$  s $^{-1}$  (the input value), and  $r_0$  fixed at 0.33, 0.34, 0.35, 0.36, 0.37 or 0.38. All other parameters, except  $\alpha$ , were fixed at the same standard values as for the previous fits. In this case,  $\alpha$  is the only parameter adjusted in the fitting process. Fig. 4 presents  $\chi_r^2$  vs. assumed fixed value of  $r_0$  for fits of the same FPA data as in Fig. 3, but now with  $\alpha$  as the only adjustable parameter. The results for  $\chi_r^2$  vs.  $r_0$ , and  $\alpha$  vs.  $r_0$  are very similar to those in Fig. 3, and the conclusions are the same. Specifically, there is no *significant* variation of  $\chi_r^2$  above 1.10, except when  $r_0=0.33$  and input  $\alpha=8.0 \times 10^{-12}$  dyn cm. Again, the best-fit value of  $\alpha$  varies strongly with the assumed fixed  $r_0$  in the fitting protocol in a manner very similar to that in Fig. 3. It is inferred from these results that fixing  $L$ ,  $R_H$  and  $D_{\perp}$  at their correct input values still does *not* make it possible to determine both  $r_0$  and  $\alpha$  in a statistically significant manner for a 24 bp DNA, and that without an independent and rather accurate knowledge (or guess) of the pertinent value of  $r_0$  for the particular DNA studied, the error in the best-fit value of  $\alpha$  is likely to be rather large.

The preceding conclusions are based on data acquired with a perfect instrument comprising perfect and perfectly aligned polarizers with perfectly calibrated relative efficien-

cies of the detection channels for parallel and perpendicularly polarized light, a negligibly small aperture, a perfect monochromator, a complete absence of any stray Rayleigh or Raman scattered light from the sample, or fast fluorescence from any filters used, and perfect electronics. In addition, the “sample” exhibits no non-intercalated dye of any kind, and no dimerization or other aggregation. Imperfections in real instruments and real samples will make the task of determining both  $r_0$  and  $\alpha$  for a 24 (or 27) bp DNA with an instrument like that of Pedone et al. [1,2] even more difficult. This difficulty persists even for an instrument with much higher time-resolution, as indicated below.

### 2.3. Fitting FPA data for a real 24 bp DNA

Attempts to determine both  $r_0$  and  $\alpha$  for a real 24 bp DNA with the sequence GCCGTCGG CAGCGACCGGCTCGGC by fitting FPA data taken in our laboratory were generally unsuccessful in ways already seen with the synthetic data. The sample contained  $3.15 \times 10^{-5}$  M duplexes and 1 ethidium per 500 bp in 100/10/1 NaCl/Tris/EDTA, pH 8.5, 293 K. Excess single strands and incomplete duplexes were removed by hydroxyapatite chromatography, and analytical gels gave *no* evidence of either failure sequences (in “denaturing” gels) or incomplete duplex structures (in “native” gels). Twelve measurements were performed, four at each of three time spans (36, 71, and 120 ns). The FWHM of the instrument function,  $e(t)$ , was <80 ps. The experimental sum function  $s(t)$  in Eq. (3) is the convolution of  $e(t)$  with the theoretical sum function ( $S(t)$ ), which in this case was taken to be a delta function ( $\delta(t)$ ) with adjustable amplitude.  $A_s$ , to account for stray light, plus two exponentials with adjustable amplitudes and time constants to account for intercalated and non-intercalated dye. The latter accounted for less than 0.5% of the total light contributed by the two exponentials. Similarly, the experimental difference function in Eq. (4) is the convolution of  $e(t)$  with the product of  $S(t)$  and the theoretical difference function ( $D(t)$ ), which in this case is taken to be  $D(t)=S(t) \cdot r(t)+r_s A_s \delta(t)$ , where  $r_s$  is the adjustable anisotropy of the stray light.

When  $r(t)$  was fitted to the experimental data by adjusting  $r_0$ ,  $R_H$ , and  $r_s$  for different assumed fixed values of  $\alpha$ , while holding constant all other parameters ( $L=84.3$  Å,  $D_{\perp}=6.493 \times 10^6$  s $^{-1}$ , and the standard parameters in Table 1), the  $\chi_r^2$  value was found to vary *insignificantly* from  $(1.00 \pm 0.05$  to  $1.01 \pm 0.05$  to  $1.02 \pm 0.05)$ , as the assumed fixed value of  $\alpha$  was increased from  $(3.00$  to  $5.90$  to  $9.00) \times 10^{-12}$  dyn cm, respectively. The notation,  $1.01 \pm 0.05$ , means that the average of the 12  $\chi_r^2$ -values (one for each data set), is 1.01, and that the standard deviation among those same 12 values is 0.05. Results of this fitting protocol (denoted by A) are listed in Table 3. Again, we find no *statistically significant* preference for any one value of  $\alpha$  over any other within this 3-fold range. The corresponding

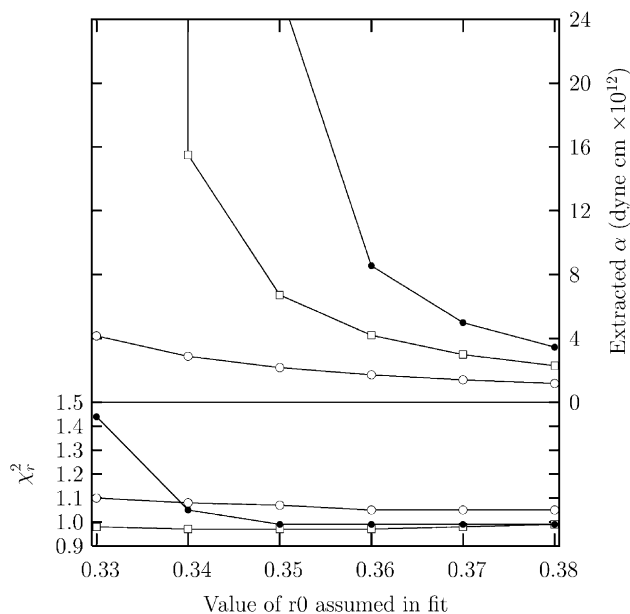


Fig. 4.  $\chi_r^2$  and best-fit  $\alpha$ -value from fits to three sets of simulated FPA data (with Poisson noise) vs.  $r_0$ -value assumed in the fit. The three sets of simulated data are the same as in Fig. 3, and differ only in the value of  $\alpha$  used to create them. In the fit,  $\alpha$  is the *only* adjustable parameter, while  $R_H$ ,  $L$ , and all other parameters except  $r_0$  are held fixed at their input values. Four of the best-fit values of  $\alpha$  are too large to be plotted on this figure. For the data simulated with  $\alpha=4.5 \times 10^{-12}$ , the best-fit  $\alpha$  for an assumed  $r_0=0.33$  is  $6.0 \times 10^{-1}$  dyn cm. For the simulated data with  $\alpha=8.0 \times 10^{-12}$ , the best-fit  $\alpha$ -values are  $1.3 \times 10^{-4}$  dyn cm for assumed  $r_0=0.33$ ,  $3.4 \times 10^{-1}$  dyn cm for assumed  $r_0=0.34$ , and  $2.58 \times 10^{-11}$  dyn cm for assumed  $r_0=0.35$ .

Table 3

Results of fitting experimental FPA for a 24 bp DNA by using protocols A, B, and C

Protocol	$\chi_r^2$	$r_0$	$R_H$ (Å)	$\alpha$ (dyn cm)	$L$ (Å)	$r_s$
A	1.00±0.05	0.393±0.004	10.1±0.1	$3.0 \times 10^{-12}$ (fixed)	84.3 (fixed)	0.33±0.06
	1.01±0.05	0.376±0.004	10.1±0.1	$5.9 \times 10^{-12}$ (fixed)	84.3 (fixed)	0.38±0.05
	1.02±0.05	0.368±0.004	10.1±0.1	$9.0 \times 10^{-12}$ (fixed)	84.3 (fixed)	0.39±0.05
B	1.00±0.05	0.387±0.009	10.1±0.1	$3.8 \pm 1.0 \times 10^{-12}$	84.3 (fixed)	0.35±0.06
C	1.00±0.05	0.390 (fixed)	10.3±0.6	$3.3 \pm 0.7 \times 10^{-12}$	82±6	0.34±0.05
	1.00±0.05	0.380 (fixed)	10.1±0.6	$4.9 \pm 1.2 \times 10^{-12}$	84±6	0.36±0.05
	1.01±0.05	0.375 (fixed)	10.0±0.6	$6.0 \pm 1.7 \times 10^{-12}$	85±6	0.38±0.05
	1.01±0.05	0.370 (fixed)	9.9±0.6	$8.9 \pm 3.4 \times 10^{-12}$	87±7	0.30±0.05
	1.01±0.06	0.365 (fixed)	9.8±0.6	$1.6 \pm 1.1 \times 10^{-11}$	88±7	0.40±0.05
	1.02±0.05	0.360 (fixed)	9.7±0.6	$7.9 \times 10^{-12}$ to $2.8 \times 10^{-4a}$	89±7	0.41±0.05

Protocols A, B, and C are described in the text. Fits were also performed for protocol C using  $r_0$  fixed at 0.355 and 0.350, for which some data sets yielded enormously unphysical torsion constants greater than 1.0 dyn cm for those fits.

<sup>a</sup> The distribution of results was highly skewed, so the range of extracted values is given instead of the average ( $3.48 \times 10^{-5}$  dyn cm) and standard deviation (which exceeds the average).

best-fit values of  $R_H$  ( $10.14 \pm 0.12$ ,  $10.08 \pm 0.11$ , and  $10.08 \pm 0.11$ ) are identical to one another within experimental error. Thus,  $R_H$  can be determined accurately by fixing  $\alpha$  anywhere in the range  $(3.0 \text{ to } 9.0) \times 10^{-12}$  dyn cm!

When  $r_0$ ,  $R_H$ , and  $\alpha$  were all taken as adjustable, the optimum value of  $\chi_r^2$  remained in the range  $1.00 \pm 0.05$ , indicating that no significant improvement in the fit could be obtained by adjusting  $\alpha$  in addition to  $r_0$  and  $R_H$ . The best-fit  $R_H$  also remained practically unchanged at  $10.11 \pm 0.13$ , as expected. The relative statistical error in the best-fit  $\alpha$  is  $\pm 26\%$  for this particular data set, but the reproducibility error (difference in best-fit  $\alpha$ ) from one set of data to the next is often much greater (data not shown). Results of this fitting protocol (denoted by B) are indicated in Table 3. Almost every set of experimental data for DNAs of a comparable size admits a unique least-squares solution for both  $r_0$  and  $\alpha$ , but the optimum values of these parameters vary greatly from one data set (with its particular Poisson noise) to another for the same system (data not shown). However, the variation in  $\chi_r^2$  among the fits is *not* statistically significant, as implied by the results for fitting protocol A, so there is no statistical basis to favor one set of optimum values over any other.

When  $r(t)$  was fitted to the same experimental data by adjusting  $\alpha$ ,  $R_H$ ,  $L$  and  $r_s$  (and calculating  $D_\perp$  by Eq. (A1) with  $\xi=1$ ) for different assumed fixed values of  $r_0$  (0.360, 0.365, 0.370, 0.375, 0.380, 0.390) and the same standard parameters in Table 1, the average  $\chi_r^2$  again varied *insignificantly* within the range from  $1.00 \pm 0.05$  to  $1.02 \pm 0.05$ , as the assumed fixed  $r_0$  was varied from 0.360 to 0.390. Results of this fitting protocol (denoted by C) are indicated in Table 3. For assumed fixed  $r_0=0.360$ , the average of the best-fit  $\alpha$ -values,  $3.48 \times 10^{-5}$  dyn cm, for the 12 data sets is unphysically large. Even for assumed fixed  $r_0=0.365$ , the average of the best-fit  $\alpha$ -values,  $16.1 \times 10^{-12}$  dyn cm, significantly exceeds the largest value obtained for any DNA by FPA ( $11.8 \times 10^{-12}$  dyn cm [36]) or by any other method ( $14.1 \times 10^{-12}$  dyn cm [37]), and is surely too large [38–41]. However, for assumed fixed  $r_0$ -values in the

range (0.370 to 0.390) the best-fit  $\alpha$ -values lie in the range  $((8.88 \text{ to } 3.34) \times 10^{-12}$  dyn cm) as expected from the above results for protocol A in Table 3. These observations suggest that  $r_0 \geq 0.370$  for this DNA, and that use of fixed  $r_0=0.360$  most likely substantially overestimates  $\alpha$  for some of the data sets.

We conclude that, for DNAs as short as 24 bp,  $r_0$  and  $\alpha$  cannot *both* be reliably retrieved by fitting data acquired with an instrument whose time resolution is comparable to that of Pedone et al., even when all model parameters except for  $r_0$  and  $\alpha$  are known accurately in advance. Even with much superior time resolution,  $<80$  ps, and a more highly purified sample that is 19-fold more dilute, and correspondingly less prone to dimerization, it was not possible to determine unique values for both  $r_0$  and  $\alpha$ . However, it was possible to rule out certain values of  $r_0$ , as indicated below.

#### 2.4. Values of $r_0 \leq 0.365$ are ruled out for our 24 bp DNA

The assumed fixed value,  $r_0=0.360$ , could be ruled out, because best-fit  $\alpha$ -values for 8 of the 12 data sets analyzed exceed  $15 \times 10^{-12}$  dyn cm, which exceeds the largest  $\alpha$ -value obtained previously for any DNA by any method. Moreover, four of those eight values exceed  $72 \times 10^{-12}$  dyn cm, which is absurdly large, and three of those exceed  $8970 \times 10^{-12}$  dyn cm, which is much larger still. The slightly higher assumed fixed value,  $r_0=0.365$ , can most probably also be ruled out, because the corresponding best-fit  $\alpha$ -values for 5 of the 12 data sets also exceed  $15 \times 10^{-12}$  dyn cm. By applying this criterion (that best-fit  $\alpha$ -values should not exceed  $15 \times 10^{-12}$  dyn cm) the acceptable range of assumed fixed  $r_0$  is 0.370–0.39. This example provides an instructive demonstration that  $r_0$  is *not* precisely 0.360 for *all* 24 bp DNAs, contrary to the assumption of Pedone et al. [1,2]. It also shows that the choice of assumed fixed  $r_0=0.360$  in this case causes half of the best-fit  $\alpha$ -values to be too large, some of them by several orders of magnitude. Additional fits of the same FPA data were performed for assumed fixed  $r_0=0.355$  and 0.350. In those cases, some of



the data sets yielded grossly unphysical best-fit  $\alpha$ -values greater than 1.0 dyn cm.

### 2.5. Why no absurdly large values were observed by Pedone et al.

There arises the question of why Pedone et al. apparently observed no absurdly large values of  $\alpha$  by fitting their data with the assumed fixed  $r_0=0.360$  [1,2]. The primary reason is that the effects of dynamic bending were neglected in their fitting protocol. In order to compensate for this neglect of depolarization due to dynamic bending, either the best-fit ARF must lie below its actual value, so as to provide an *extra* amplitude of dye wobble, or the best-fit value of  $\alpha$  must be only about 2/3 (or less) of its actual value to provide an *extra* amplitude of twisting. As the assumed fixed ARF-value is decreased *below* its actual value, corresponding to a larger amplitude of dye wobble, then a smaller *excess* amplitude of twisting is required, and the best-fit  $\alpha$ -value rises, at first from about 2/3 of its actual value toward its actual value. Finally for still greater decreases in the assumed fixed ARF-value, the best-fit  $\alpha$ -value rises above its actual value. In contrast, when the effects of dynamic bending are taken into account in the fitting protocol by assuming fixed  $P_d=1800$  Å, the best-fit  $\alpha$ -value rises above its actual value as soon as the assumed fixed ARF-value is decreased below its actual value, and reaches much higher values for the same decrease in assumed fixed ARF-value than is the case when no account is taken of dynamic bending. If a slightly lower  $r_0$  value, such as  $r_0=0.350$ , had been selected by Pedone et al. [1,2], then absurdly large best-fit  $\alpha$ -values would likely have been observed for some samples, despite their neglect of dynamic bending.

### 2.6. Variations in $R_H$ and $L$

Our usual protocol (denoted by A in Table 3) for fitting FPA data from DNAs containing 12 to 36 bp is to fix  $\alpha$  at one or more suitable values in the range  $(3 \text{ to } 9) \times 10^{-12}$  dyn cm, to fix  $L=Nh+2.7$  Å, and to fix all other parameters at appropriate standard values like those in Table 1, and to adjust  $r_0$  and  $R_H$ . The values of  $R_H$  obtained in this way are very insensitive to the choice of  $\alpha$ , as seen for protocol A in Table 3.

For a collection of eight different experimental DNAs containing 12(3x), 16, 24, and 36(3x) bp, *all* of the average best-fit  $R_H$ -values lie in the range  $10.0 \pm 0.2$  Å [7], as observed for the 24-mer in Table 3 (protocol A). This, we believe, is the correct range for such short DNAs.

Pedone et al. employed a different protocol, wherein  $r_0$  was fixed at 0.36, while  $\alpha$ ,  $R_H$ , and  $L$  were all taken as adjustable [1,2]. They did not report the  $R_H$  and  $L$  values in their recent study of forty-three 24 bp DNAs [1], but in their earlier study of ten 27 bp DNAs, the best-fit  $R_H$ - and  $L$ -values (obtained from the rise per bp,  $h$ ) were reported for each DNA [2]. The  $R_H$ -values ranged from 10.8 to 11.8 Å

and are not obviously correlated with  $\alpha$ . It appears that the best-fit  $R_H$  values are all significantly (1.08- to 1.13-fold) too large and that the spread among them ( $\sim 1$  Å) is also too great. Both of these results are well outside the ranges that we have found for such short DNAs via protocol A. Best-fit experimental  $L$ -values are reckoned from the reported best-fit rises per base pair ( $h$ ) [2] according to  $L=(27)h$  Å. These  $L$ -values span the range from 78.3 (for  $h=2.9$  Å) to 91.8 (for  $h=3.4$  Å), and are not obviously correlated with  $\alpha$ . It appears that the reductions in effective length below 94.5 Å are much too great for many of these DNAs, and that the spread in effective lengths among these DNAs is also too great. The effect of equilibrium rms curvature is to decrease the effective length of such short DNAs by only  $\sim 1\%$  (determined by fits to noise-free data), yet the observed range of reductions (from 94.5 Å) extends from 0.97- to 0.85-fold. The overestimation of  $R_H$  and underestimation of  $L$ , and also the unanticipated spreads among both  $R_H$  and  $L$  appear to be incompatible with the model of Pedone et al., as discussed in the following section. Evidently, the choice of  $r_0$  as a fixed parameter in the fit violates criterion (d) of Introduction. Together with the foregoing analyses, this demonstrates that fixing  $r_0$  violates all of the stated criteria for a reasonable choice of such a fixed parameter.

### 2.7. Comparison of the model of Pedone et al. with the reported values of $R_H$ and $L$

According to the *model of Pedone et al.*, the 53 DNAs *all* exhibit precisely the same value  $r_0$  (0.360), but a range of  $\alpha$ -values. FPA data for 27 bp DNAs were simulated using  $r_0=0.360$  and each of a series of  $\alpha$ -values spanning the range from  $(1.5 \text{ to } 9.0) \times 10^{-12}$  dyn cm in steps of  $0.5 \times 10^{-12}$  dyn cm. The other input values were  $R_H=10.0$  Å,  $L=94.5$  Å, and the standard parameters in Table 1. The instrument function was taken to be a Gaussian with 7 ns FWHM to represent the time-resolution of the 40 MHz frequency domain instrument. Poisson noise was added to the computed FPA data as before. In the fitting protocol, we fix  $r_0=0.360$ , and adjust  $\alpha$ ,  $R_H$ , and  $L$ , while holding all other parameters at their input values, except for  $P_d$ , which is assumed to be  $P_d=\infty$ . Also, no account is taken of the slight reduction in effective length due to the equilibrium persistence length,  $P_{eq}=500$  Å. Because this effect is incorporated into the *simulated* FPA data, the best-fit effective length *in the absence of noise* is  $L=93.6$  Å, about 1% less than the input value. This fitting protocol corresponds to that of Pedone et al. [1,2].

The best-fit-values of  $R_H$  and  $L$  typically lie within one standard deviation of their expected input values, but the best-fit  $\alpha$  is only about 2/3 of its input value in nearly all cases, except for the particular input value of  $2.0 \times 10^{-12}$  dyn cm. The results for input  $\alpha=(2.0 \text{ to } 5.9) \times 10^{-12}$  dyn cm are shown in Table 4. This  $\sim 0.66$ -fold discrepancy between typical best-fit and input values of  $\alpha$  is due primarily to neglecting the effects of dynamic bending in the fitting

Table 4

Summary of best-fit values extracted from FPA data simulated according to the model of Pedone et al., and from experimental phase and modulation data

	$\alpha$ ( $10^{-12}$ dyn cm)	$R_H$ (Å)	$L$ (Å)
Extracted from simulated FPA data <sup>a</sup>	1.71 to 3.96	$10.2 \pm 0.1$	$91.4 \pm 1.3$
Extracted from phase and modulation measurements [2] <sup>b</sup>	2.3 to 5.3	$11.0 \pm 0.3$	$85.1 \pm 4.2$

<sup>a</sup> The first row presents average best-fit values obtained from FPA data that were simulated using input  $\alpha$ -values in the range  $(2.0 \text{ to } 5.9) \times 10^{-12}$  dyn cm, and input values of the other parameters:  $r_0=0.360$ ,  $N+1=28$ ,  $R_H=10.0$  Å,  $L=94.5$  Å,  $P_d=1800$  Å,  $\varepsilon=70.5^\circ$ ,  $T=293$  K,  $\eta=0.01002$  P, and  $D_\perp=6.493 \times 10^6$  s<sup>-1</sup>. The instrument function was a Gaussian with 7 ns width. For each choice of simulated parameters (i.e. for each input value of  $\alpha$ ), three different FPA data sets were generated by the addition of Poisson noise to the calculated  $i_{||}(t)$  and  $i_\perp(t)$ . For the least squares fits,  $r_0$  was held fixed at 0.360 and  $P_d$  was assumed to be infinite, while  $\alpha$ ,  $R_H$ , and  $L$  were varied, as described in the text. On each iteration of the fitting protocol,  $D_\perp$  was calculated from the current trial values of  $R_H$ , and  $L$  according to Eq. (A1) with  $\xi=1.0$ . The table shows the range of average best-fit  $\alpha$ -values, and the average best-fit values and standard deviations of  $R_H$  and  $L$  for the simulated data sets.

<sup>b</sup> The second row indicates the range of best-fit  $\alpha$ -values and the average best-fit values and standard deviations of  $R_H$  and  $L$  reported by Pedone et al. for ten 27 bp DNAs [2].

protocol [1,2]. One consequence of this reduction in  $\alpha$  is that an input  $\alpha$ -value as high as  $9.0 \times 10^{-12}$  dyn cm barely suffices to yield the maximum experimental value,  $\alpha=5.3 \times 10^{-12}$  dyn cm, obtained for the set of ten 27 bp DNAs, and fails to yield the maximum experimental value,  $7.9 \times 10^{-12}$  dyn cm, obtained for the forty-three 24 bp DNAs. The relative statistical errors are ~2% in  $R_H$  and  $L$  and ~5–10% in  $\alpha$ . The 0.66-fold systematic discrepancy clearly dominates the statistical error in  $\alpha$ .

The average experimental values reported by Pedone et al. [2] are also indicated in Table 4. The average of the experimental  $R_H$ -values,  $\langle R_H \rangle = 11.05 \pm 0.33$  Å, exceeds what we believe to be the correct value ( $10.00 \pm 0.2$  Å) by ~10% [2]. The spread of the best-fit experimental  $R_H$ -values among the different samples is taken to be the standard deviation about the mean of those same values. The ratio of spreads of the  $R_H$ -values for the experimental and simulated samples is  $\sim 0.33/0.13=2.54$ , which significantly exceeds 1.0. The experimental values of Pedone et al. for the rise per bp yield an average length for a 27 bp DNA,  $\langle L \rangle = 85.1 \pm 4.2$  Å. This  $\langle L \rangle$  lies below the expected value,  $L=0.99(27)(3.4)+2.7=93.6$  Å by ~9%, and the ratio of the spreads of the experimental and synthetic values,  $4.2/1.5=2.8$ , also significantly exceeds 1.0. Unless these short DNAs are all very highly curved, there is no plausible reason for the experimental  $R_H$  to systematically exceed its expected value by so much, or for  $L$  to systematically underlie its expected value by so much. Also, the spreads among the experimental  $R_H$ - and  $L$ -values are also much greater than predicted by the model. It may be concluded that the model of Pedone et al. (wherein all DNAs exhibit

$r_0=0.360$ , but different values of  $\alpha$ ) does not adequately mimic the experimental results for  $R_H$  and  $L$ .

## 2.8. Comparison of an alternative model with the reported $R_H$ and $L$

We now consider an alternative model, wherein all DNAs possess the same value of  $\alpha$ , but different values of  $r_0$ . This model lies at the opposite extreme from that of Pedone et al., wherein all DNAs possess the same  $r_0$ , but different  $\alpha$ . Although real DNAs surely lie between these two extremes, it is instructive to ask which extreme model best accounts for the experimental results of Pedone et al. It is important to ascertain the origins of the peculiar results reported for  $R_H$  and  $L$ .

FPA data were simulated using a single input value,  $\alpha=5.9 \times 10^{-12}$  dyn cm, for all DNAs, but different input  $r_0$ -values, which span the range from 0.325 to 0.380 in steps of 0.005. The simulation protocol and all other input parameters are precisely the same as in the preceding section, and the fitting protocol with assumed fixed  $r_0=0.360$  and adjustable  $\alpha$ ,  $R_H$ , and  $L$  is also identical. This model provides ranges of best-fit  $\alpha$ -values,  $R_H$ -values, and  $L$ -values that overlap the corresponding experimental data for both 27 bp and 24 bp DNAs (data not shown). In that sense, it provides better agreement with the experimental results for  $R_H$  and  $L$ . However, it also predicts a significant correlation of the larger best-fit  $R_H$ -values with the smaller  $L$ -values and  $\alpha$ -values, which is not reflected in the experimental data. Although this model provides a better overall match to the experimental results, neither this model nor that of Pedone et al. captures the fact that the best-fit reported  $R_H$ -values all exceed 10.7 Å. This circumstance suggests the presence of some additional systematic error. One possibility is that the detection efficiency of the “ $\perp$ ” channel of the frequency-domain instrument exceeds that of the “ $||$ ” channel by ~0.6%. Factory calibration of the so-called g-factor, which characterizes the ratio of detection efficiencies of the two channels is stated to be accurate to within  $\pm 0.8\%$ . We can simulate the effects of such a small systematic error simply by scaling  $I_{||}(t)$  by 0.994 prior to fitting. This corresponds to a 0.6% error, within the allowed range.

This systematic error is incorporated into the simulated FPA data for the model of Pedone et al., and those data are fitted in the same way as before with assumed fixed  $r_0=0.360$  (data not shown). This slight downscaling of  $i_{||}(t)$  (relative to  $i_\perp(t)$ ) causes a (further) reduction in the best-fit  $\alpha$ -values by  $(0.83 \pm 0.12)$ -fold. Consequently, even for a rather large input value,  $\alpha=9.0 \times 10^{-12}$  dyn cm, the corresponding best-fit  $\alpha$ -value,  $4.40 \times 10^{-12}$  dyn cm, lies significantly below the maximum experimental values,  $((5.3 \text{ and } 7.9) \times 10^{-12})$  dyn cm, obtained for the 27 and 24 bp DNAs, respectively [1,2]. Also, for input  $\alpha \leq 2.5 \times 10^{-12}$  dyn cm, the best-fit  $\alpha$ -values lie well below the lowest

experimental values,  $(2.3 \text{ and } 1.8) \times 10^{-12}$  dyn cm, reported for 27 and 24 bp DNAs, respectively.

For input  $\alpha$ -values in the range  $(9.0 \text{ to } 3.0) \times 10^{-12}$  dyn cm, the best-fit  $R_H$ -values lie in the range 10.4 to 10.9 Å, which contains 5 of the 10 experimental values. However, in order to attain  $R_H$ -values as high as the other five experimental values (11.0 to 11.8 Å), the best-fit  $\alpha$ -values would have to lie significantly below the lowest experimental value ( $2.3 \times 10^{-12}$  dyn cm) reported for any of the ten 27 bp DNAs.

Best-fit  $L$ -values lie in the narrow range 87.2 to 82.9 Å for all input  $\alpha$ -values from  $(9.0 \text{ to } 3.0) \times 10^{-12}$  dyn cm. In particular, no  $L$ -values are found to be as high as the 91.8 Å found for 2 of the 10 experimental DNAs, or as low as the 3 lowest values (78.3, 81.0 and 81.0 Å) among those 10 DNAs.

We conclude that downscaling  $I_{||}(t)$  actually worsens the overall agreement between the *model of Pedone et al.* and the experimental data.

The same systematic error is incorporated into the simulated FPA data for the *alternative model*, and those data are fitted in the same way as before with assumed fixed  $r_0=0.360$  to obtain the results in Table 5. This slight downscaling of  $I_{||}(t)$  causes  $(0.82 \pm 0.07)$ -fold reductions in best-fit  $\alpha$ , virtually the same as for the model of Pedone et al.

Now, as the input  $r_0$  is decreased from 0.370 to 0.350,  $\alpha$  declines monotonically from  $(5.3 \text{ to } 2.25) \times 10^{-12}$  dyn cm, which closely matches the experimental span  $(5.3 \text{ to } 2.3) \times 10^{-12}$  dyn cm for the ten 27 bp DNAs. Over the range of input  $r_0$  from 0.365 to 0.340, the best-fit  $R_H$  precisely covers the experimental range, 10.7 to 11.8 Å, and over the range of input  $r_0$  from 0.37 to 0.335, the best-fit  $L$ -

values extend from 89.4 to 77.1 Å, which also nearly covers the experimental span (91.8 to 78.3 Å). Thus, this alternative model with the single input  $\alpha=5.9 \times 10^{-12}$  dyn cm and a range of input  $r_0$ -values *within the previously observed range*, together with a slight error in the factory calibrated g-factor within its allowed range, is capable of producing nearly all of the experimental values of  $\alpha$ ,  $R_H$ , and  $L$ . There still is predicted a significant correlation between larger  $R_H$  values and smaller  $\alpha$ - and  $L$ -values that is not evident in the experimental data for the ten 27 bp DNAs. This may indicate that other sources of variability in the data, or other factors, including some modest variation in the actual  $\alpha$ -values among the different DNAs, are also involved.

Although this comparison with the experimental data by no means proves that any error in the g-factor prevails in the experiments of Pedone et al., it is consistent with that possibility.

The  $\sim 0.82$ -fold reductions in best-fit  $\alpha$  for either model, which arise from a 0.6% error in g-factor, provide another example of the extreme sensitivity of best-fit  $\alpha$  to spurious factors in the case of such short DNAs, *whenever  $r_0$  is assumed fixed at 0.360*. In contrast, for much longer DNAs, where both  $r_0$  and  $\alpha$  can be determined reliably, a 0.994 downscaling of  $I_{||}(t)$  causes only a  $\sim 2\%$  reduction in the best-fit  $\alpha$  and a  $\sim 0.5\%$  decrease in  $r_0$ .

## 2.9. Conclusions regarding the reported $\alpha$ -values

The foregoing considerations and analyses indicate that: (1) DNAs with very ( $\sim 5$ -fold) different  $\alpha$ -values and slightly ( $\sim 10\%$ ) different  $r_0$ -values can have  $r(t)$  curves that are very nearly identical for all  $t \geq 1$  ns; (2) for DNAs containing 24 bp,  $\alpha$  and  $r_0$  cannot be simultaneously assessed using an instrument with a time resolution of 7 ns, or even  $< 80$  ps; (3)  $r_0$  is not always 0.360, but varies over a considerable range (0.31 to 0.38); (4) small relative errors ( $\leq 10\%$ ) in  $r_0$  can cause enormous (several-fold) errors in the best-fit  $\alpha$ -values; (5) the 4.4-fold span of experimental  $\alpha$ -values reported by Pedone et al. can be obtained from data that are simulated using a *single* typical input  $\alpha$ -value and various input  $r_0$ -values within the reasonable range, 0.370 to 0.340, by fitting those data according to the protocol of Pedone et al. (i.e. with assumed fixed  $r_0=0.360$ ); and (6) when the simulated  $I_{||}(t)$  are systematically downscaled by 0.994, this latter model provides much better overall agreement with the experimental results for  $R_H$  and  $L$  than does the model of Pedone et al. [1,2]. This suggests that variations in  $r_0$  among the different DNAs are more significant than variations in  $\alpha$ , but does not preclude modest variations in  $\alpha$ . We conclude that many, if not all, of the 53  $\alpha$ -values reported by Pedone et al. are likely to contain substantial systematic errors. Such systematic errors vary from one sample to another in both magnitude and direction, depending upon their unknown  $r_0$ -values, so neither the relative values, nor the 4.4-fold spread among those, nor the average of all 53 such values would be

Table 5

Results of fitting simulated FPA data for 27 bp DNAs plus one intercalated ethidium with different input  $r_0$ -values, and with 0.994 scaling of  $i_{||}(t)$ , but fitted with fixed  $r_0=0.360$

Simulated $r_0$	$\alpha$ ( $10^{-12}$ dyn cm)	$R_H$ (Å)	$L$ (Å)
0.335	$1.49 \pm 0.14$	$11.7 \pm 0.7$	$78.6 \pm 4.2$
0.340	$1.66 \pm 0.08$	$11.8 \pm 0.2$	$77.1 \pm 1.1$
0.345	$2.09 \pm 0.14$	$11.2 \pm 0.1$	$81.0 \pm 0.5$
0.350	$2.25 \pm 0.14$	$11.2 \pm 0.4$	$81.2 \pm 3.1$
0.355	$2.82 \pm 0.20$	$10.8 \pm 0.3$	$84.0 \pm 1.7$
0.360	$3.56 \pm 0.37$	$10.7 \pm 0.2$	$85.0 \pm 1.4$
0.365	$3.82 \pm 0.08$	$10.8 \pm 0.2$	$84.4 \pm 1.8$
0.370	$5.29 \pm 0.48$	$10.2 \pm 0.2$	$89.4 \pm 2.4$

Each line is obtained by fitting three different sets of FPA data that were simulated with the indicated value of  $r_0$ . The other parameters used to simulate the FPA data were:  $(N+1)=28$ ,  $\alpha=5.9 \times 10^{-12}$  dyn cm,  $R_H=10.0$  Å,  $L=94.5$  Å,  $D_{\perp}=6.493 \times 10^{-3}$  ns $^{-1}$ ,  $P_d=1800$  Å,  $\varepsilon=70.5^\circ$ ,  $T=293$  K, and  $\eta=0.01002$  P. The instrument function was a Gaussian with 7 ns width. The theoretical  $i_{||}(t)$  was scaled by 0.994. Poisson noise was included in the simulated data, and three different simulated data sets were generated for each value of  $r_0$ . For the least squares fits,  $r_0$  was held fixed at 0.360 and  $P_d$  was assumed to be infinite, while  $\alpha$ ,  $R_H$ , and  $L$  were varied, as described in the text. On each iteration of the fitting protocol,  $D_{\perp}$  was calculated from the current trial values of  $R_H$  and  $L$  according to Eq. (A1) with  $\xi=1.0$ . The table shows the average and standard deviations of the best-fit values of  $\alpha$ ,  $R_H$ , and  $L$  for each simulated data set.



expected to remain unaffected, in the event that such errors could be corrected.

Superimposed on the preceding variable systematic errors is a more uniform systematic error that stems from neglecting the effects of dynamic bending, and which acts to reduce the best-fit  $\alpha$  by  $\sim 0.66$ -fold below what it would be otherwise.

In the absence of precise independent measurements of  $r_0$  in each case, none of the 53 reported  $\alpha$ -values for 24 and 27 bp DNAs [1,2] can be regarded as experimentally justified. In particular, the relative variations in  $\alpha$  among the different sequences almost certainly contain substantial, if not dominant, contributions from modest variations in their actual  $r_0$ -values, so the 4.4-fold spread among the reported  $\alpha$ -values is most likely much too large. For those 24 or 27 bp sequences, whose actual  $r_0$ -values lie below 0.360, the reported  $\alpha$ -values are 0.66-fold too low or lower, due to the failure to account for effects of dynamic bending. For the longer calf-thymus DNA, the reported  $\alpha$ -value is about 0.76-fold too low for the same reason [33].

It is not only conceivable but likely that variations among the reported best-fit  $\alpha$ -values of Pedone et al. arise more from variations among the actual  $r_0$ -values of the different DNAs than from variations among their actual  $\alpha$ -values. In other words, the reported  $\alpha$ -values may be better correlated with stiffness against libration of the intercalated dye than with stiffness against twisting.

#### 2.10. Validity of the elastic constants for reported for 136 tetranucleotide steps

The 53 DNAs were reported to contain collectively all 136 distinct tetranucleotide steps. The measured torsion elastic constant of each DNA was expressed in terms of the torsion elastic constants of the central dinucleotide steps of each of its overlapping interior tetranucleotide sequences plus the dinucleotide steps at its ends, all of which are assumed to be independent of any longer range sequence context. The end-step values were fixed by assumption. A genetic algorithm was employed to determine the value of the torsion elastic constant associated with the central dinucleotide step of each of the 136 possible tetranucleotide steps. This algorithm varied the 136 trial torsion elastic constants, so as to reduce the sum of squared differences between the calculated and measured values for the 53 DNAs below some unspecified target value. This problem is equally well formulated as a least-squares minimization problem, wherein a set of 53 measured values is fitted by adjusting 136 parameters. Because this problem is enormously underdetermined, a unique solution normally does not exist. Instead, there are usually infinitely many choices of the parameters that yield the same minimum value of the sum of squared differences. Because the minimum value was not reached, there are likely even more possible solutions compatible with the data. The only circumstance, wherein a *unique* least-squares solution could result is one, wherein

the system actually follows a simpler model, such as a dinucleotide model, that is subsumed by the tetranucleotide model, but which is characterized by  $n \leq 53$  parameters. Thus, any claim to have determined a unique solution for all 136 tetranucleotide sequences by fitting only 53 measured values for different DNA sequences necessarily also implies that the system does not follow the full tetranucleotide model, but instead follows a subsumed simpler model with sufficient redundancy among the torsion elastic constants of different tetranucleotides to reduce the number of relevant adjustable parameters from 136 to 53 or less.

Serious objections can be raised against the torsion elastic constants reported by Pedone et al. for the 136 tetranucleotide sequences [1]. First, the 53 reported torsion elastic constants, from which the 136 tetranucleotide values were extracted, are themselves unreliable, and most likely contain large and variable systematic errors, as noted above. Indeed, variations among those 53 reported torsion elastic constants are more likely to be correlated with variations among the actual  $r_0$ -values than with variations among the actual  $\alpha$ -values of those 53 DNAs. In such a case, Eq. (3) of Pedone et al. would not apply, and the genetic algorithm would have fitted an inapplicable relation to the experimental data. Second, it is highly doubtful that the torsion elastic constants obtained for the 136 tetranucleotide steps constitute a unique solution to the least-squares problem. No evidence is presented that the genetic algorithm has reached any kind of a minimum in the sum of squared differences, much less the true minimum. On three successive runs of the genetic algorithm beginning with *uniform* trial values ( $\alpha = 2$  or 5 or 8)  $\times 10^{-12}$  dyn cm, about 116 of the tetranucleotide  $\alpha$ -values came to nearly the same final values but about 20 came to significantly different values [1]. Moreover, upon adding the measured torsion elastic constants of 10 additional sequences to the set of 53, the genetic algorithm became “unstable.” These observations are particularly difficult to reconcile with any notion that the 136 reported values constitute a unique solution to the least-squares problem. If no unique solution exists, then the problem is underdetermined and infinitely many equally probable solutions must exist. Finally, substantial evidence for long range effects of certain sequences, especially alternating (CG) $_n$ , on the structure and torsion elastic constant of their flanking DNA has been reported [42,43]. Such behavior indicates a failure of simple dinucleotide or tetranucleotide models for certain sequences. In the absence of any more substantial supporting evidence, the 136 reported values of the torsion elastic constants for the different tetranucleotide sequences [1] cannot be taken seriously.

#### Acknowledgement

This work was supported in part by a grant R01 GM61685 from the National Institutes of Health.



## Appendix A

The diffusion coefficient for uniform rigid body rotation around a transverse axis perpendicular to the symmetry axis is given by [20]

$$D_{\perp} = \xi 3k_B T (\ln p + \delta_{\perp}) / (\pi L^3 \eta) \quad (\text{A1})$$

where  $k_B$  is Boltzman's constant,  $L = Nh + 2.7 \text{ \AA}$  is the contour length of an  $N$  bp DNA with rise per bp  $h$  that contains one intercalated ethidium,  $p = L/(2R_H)$  is the axial ratio,  $\eta$  is the solvent viscosity,  $\delta_{\perp}$  is given by [17]

$$\delta_{\perp} = -0.662 + (0.917/p) - 0.050/p^2 \quad (\text{A2})$$

and  $\xi$  is a scale factor that takes into account the slight reduction in end-to-end distance due to spontaneous curvature appropriate for an *equilibrium* persistence length,  $P_{\text{eq}} = 500 \text{ \AA}$ . This scale factor is reckoned by the method of Hagerman and Zimm for DNAs of different length and extrapolated to the length,  $L = (N+1)h$ . For  $N+1=25$ , it is found that  $\xi = 1.017$  [44]. In the present application this scale factor is practically inconsequential, and is included mainly for completeness, and to maintain consistency with our treatment of somewhat longer DNAs [17,36].

The diffusion coefficient for uniform rigid body rotation around the symmetry axis is given by

$$D_{\parallel} = k_B T / [(3.841)(1 + \delta_{\parallel}) \pi R_H^2 L \eta] \quad (\text{A3})$$

where

$$\delta_{\parallel} = 1.119 \times 10^{-4} + (0.6884/p) - (0.2019/p^2). \quad (\text{A4})$$

The friction factor per bp for aximuthal rotation about the symmetry axis is

$$\gamma = f_{\parallel} / (N+1) = (3.841)(1 + \delta_{\parallel}) \pi R_H^2 h \eta \quad (\text{A5})$$

The theoretical anisotropy function is given by [16]

$$r(t) = r_0 \sum_{n=0}^2 I_n C_n(t) F_n(t) \quad (\text{A6})$$

wherein  $r_0 = (0.4)(\text{ARF})$ , the amplitude reduction factor is

$$\text{ARF} = \langle P_2(\cos \beta_F) \rangle \quad (\text{A7})$$

and  $\beta_F$  is the angle between the transition dipole and its minimum energy position which in turn makes an angle  $\varepsilon_0 = 70.5^\circ$  with the helix-axis.

$$I_0 = [(3/2)\cos^2 \varepsilon_0 - 1/2]^2 \quad (\text{A8a})$$

$$I_1 = 3\cos^2 \varepsilon_0 \sin^2 \varepsilon_0 \quad (\text{A8b})$$

$$I_2 = (3/4)\sin^4 \varepsilon_0 \quad (\text{A8c})$$

The twisting correlation function is given by

$$C_n(t) = (N+1)^{-1} \sum_{m=1}^{N+1} \exp \left[ -n^2 \sum_{\ell=2}^{N+1} d_{\ell}^2 Q_{m\ell}^2 \left( 1 - e^{-t/\tau_{\ell}} \right) \right] \times \exp \left[ -n^2 D_{\parallel} t \right] \quad (\text{A9})$$

where

$$\tau_{\ell} = \gamma / (4\alpha \sin^2 [(\ell-1)\pi / (2(N+1))]) \quad (\text{A10})$$

is the relaxation time of the  $\ell$ th normal mode, and  $\alpha$  is the torsion elastic constant between bp.

$$d_{\ell}^2 = k_B T / (4\alpha \sin^2 [(\ell-1)\pi / (2(N+1))]) \quad (\text{A11})$$

is the mean squared amplitude of the  $\ell$ th normal mode.

$$Q_{m\ell} = (1 - \delta_{\ell 1}) [2/(N+1)]^{1/2} \cos[(m-1/2)(\ell-1)\pi / (N+1)] + \delta_{\ell 1} [1/(N+1)]^{1/2} \quad (\text{A12})$$

is the projection of the  $\ell$ th normal mode onto the  $m$ th subunit (either bp or intercalated dye). The residual amplitude of  $C_n(t)$  at times  $t > \tau_2$ , after the torsional deformations have decayed always, is given by

$$C_n(t) = B_n(\infty) \exp(-n^2 D_{\parallel} t) \quad (\text{A13})$$

where

$$B_n(\infty) = (N+1)^{-1} \sum_{m=1}^{N+1} \exp \left[ -n^2 \sum_{\ell=2}^{N+1} d_{\ell}^2 Q_{m\ell}^2 \right] \quad (\text{A14})$$

In the present study, the  $C_n(t)$  are evaluated numerically by completing the sums in Eq. (A9) and/or Eq. (A14). The tumbling correlation function is given by

$$F_n(t) = \exp \left[ - (6 - n^2) D_{\perp} t - (6 - n^2) A_n \times \sum_{k=1}^{k_{\max}} \left( 1 - e^{-t/T_k} \right) / (2k+1)^2 \right] \quad (\text{A15})$$

where

$$A_n = -\ln D_n(\infty) / \left[ (6 - n^2) \sum_{k=1}^{k_{\max}} 1 / (2k+1)^2 \right] \quad (\text{A16})$$

and the bending times are given by

$$1/T_k = (k_B T P_d \kappa_k^4 / (4\pi\eta)) \left[ K_0(\kappa_k R_H) + \left( \frac{\kappa_k R_H}{2} \right) K_1(\kappa_k R_H) \right] \quad (\text{A17})$$

wherein  $\kappa_k \equiv (2k+1)\pi/2L$ ,  $P_d$  is the dynamic persistence length, and  $K_0(x)$  and  $K_1(x)$  are modified Bessel functions, and

$$D_n(\infty) = (Z_n)^{-1/2} \exp(-Z_n/3) \left( \pi^{1/2}/2 \right) \text{erf} \left( Z_n^{1/2} \right) \quad (\text{A18})$$

and  $Z_n = (6 - n^2)L/4P_d$ . The mode index  $k_{\max}$  is the largest integer beyond which the  $T_k$  begin to decrease (unphysically) with increasing  $k$ , and the sum is truncated at that point [16]. At long times,  $t \gg T_1$ , after the bending modes have decayed away, the tumbling correlation function becomes

$$F_n(t) = D_n(\infty) \exp[-(6 - n^2)D_{\perp}t] \quad (\text{A19})$$

## References

- [1] F. Pedone, F. Mazzei, D. Santoni, Sequence-dependent DNA torsional rigidity: a tetranucleotide code, *Biophys. Chem.* 112 (2004) 77–88.
- [2] F. Pedone, F. Mazzei, M. Matzeu, F. Barone, Torsional constant of 27-mer DNA oligomers of different sequences, *Biophys. Chem.* 94 (2001) 175–184.
- [3] F. Barone, G. Chirico, M. Mazzeu, F. Mazzei, F. Pedone, Triple helix oligomer melting measured by fluorescence polarization anisotropy, *Eur. Biophys. J.* 27 (1998) 137–146.
- [4] F. Barone, F. Mazzei, M. Matzeu, F. Barone, Torsional constant of 27-mer DNA oligomers of different sequences, *Biophys. Chem.* 94 (1999) 259–269.
- [5] F. Barone, L. Cellai, M. Matzeu, F. Mazzei, F. Pedone, DNA, RNA and hybrid RNA–DNA oligomers of identical sequence: structural and dynamic differences, *Biophys. Chem.* 86 (2000) 37–47.
- [6] F. Barone, F. Cellai, C. Giordano, M. Matzeu, F. Mazzei, F. Pedone, X-ray footprinting and fluorescence polarization anisotropy of a 30-mer synthetic DNA fragment with one 2'-deoxy-7-hydro-8 oxoguanosine lesion, *Eur. Biophys. J.* 28 (2000) 621–628.
- [7] B.S. Fujimoto, J.M. Miller, N.S. Ribeiro, J.M. Schurr, Rotational dynamics of short DNAs, *SPIE Proc.* 1922 (1993) 360–367.
- [8] S. Nuutero, B.S. Fujimoto, P.J. Flynn, B.R. Reid, N.S. Ribeiro, J.M. Schurr, The amplitude of local angular motion of purines in DNA in solution, *Biopolymers* 34 (1994) 463–480.
- [9] J. Duhamel, J. Kanyo, G. Dinter-Gottlieb, P. Lu, Fluorescence emission of ethidium bromide intercalated in defined DNA duplexes: evaluation of hydrodynamics components, *Biochemistry* 35 (1996) 16687–16697.
- [10] G. Chirico, M. Collini, K. Toth, N. Brun, J. Langowski, Rotational dynamics of curved DNA fragments studied by fluorescence polarization anisotropy, *Eur. Biophys. J.* 29 (2001) 597–606.
- [11] P.-G. Wu, B.S. Fujimoto, J.M. Schurr, Time-resolved FPA of short restriction fragments. The friction factor for rotation of DNA about its symmetry axis, *Biopolymers* 26 (1987) 1463–1488.
- [12] B.S. Fujimoto, J.M. Miller, N.S. Ribeiro, J.M. Schurr, Effects of different cations on the hydrodynamic radius of DNA, *Biophys. J.* 67 (1994) 304–308.
- [13] M. Collini, G. Chirico, G. Baldini, M.E. Bianchi, Conformation of short DNA fragments by modulated fluorescence polarization anisotropy, *Biopolymers* 36 (1995) 211–225.
- [14] M. Collini, G. Chirico, G. Baldini, M.E. Bianchi, Enhanced flexibility of a bulged DNA fragment from fluorescence anisotropy and Brownian dynamics, *Macromolecules* 31 (1998) 695–702.
- [15] J.M. Schurr, B.S. Fujimoto, P.-G. Wu, L. Song, Fluorescence studies of nucleic acids. Dynamics, rigidities, and structures, in: J.R. Lakowicz (Ed.), *Topics in Fluorescence Spectroscopy, Biochemical Applications*, vol. 3, Plenum Press, New York, 1993, pp. 137–229.
- [16] J.M. Schurr, B.S. Fujimoto, The amplitudes of local angular motions of intercalated dyes and bases in DNA, *Biopolymers* 27 (1988) 1543–1569.
- [17] A.N. Naimushin, B.S. Fujimoto, J.M. Schurr, Dynamic bending rigidity of a 200 bp DNA in 4 mM ionic strength, *Biophys. J.* 78 (2000) 1498–1518.
- [18] T.M. Okonogi, A.W. Reese, S.C. Alley, P.B. Hopkins, B.H. Robinson, Flexibility of duplex DNA on the sub-microsecond timescale, *Biophys. J.* 77 (1999) 3256–3276.
- [19] T.M. Okonogi, S.C. Alley, A.W. Reese, P.B. Hopkins, B.H. Robinson, Sequence-dependent dynamics in duplex DNA, *Biophys. J.* 78 (2000) 2560–2571.
- [20] M.M. Tirado, J. Garcia de la Torre, Rotational dynamics of rigid symmetric top macromolecules. Application to circular cylinders, *J. Chem. Phys.* 73 (1980) 1986–1993.
- [21] W. Bauer, J. Vinograd, Interaction of closed circular DNA with intercalative dyes: II. The free energy of superhelix formation in SV40 DNA, *J. Mol. Biol.* 47 (1970) 419–435.
- [22] J.L. Bresloff, D.M. Crothers, Equilibrium studies of ethidium–polynucleotide interactions, *Biochemistry* 20 (1981) 3547–3553.
- [23] R.B. Macgregor Jr., R.M. Clegg, T.M. Jovin, Pressure-jump study of the kinetics of ethidium bromide binding to DNA, *Biochemistry* 24 (1985) 5503–5510.
- [24] S. Chandrasekaran, R.L. Jones, W.D. Wilson, Imino 1H- and 31P-NMR analysis of the interaction of propidium and ethidium with DNA, *Biopolymers* 224 (1985) 1963–1979.
- [25] W.D. Wilson, C.R. Krishnamoorthy, Y.H. Wang, J.C. Smith, Mechanism of intercalation: ion effects on the equilibrium and kinetic constants for the interaction of propidium and ethidium with DNA, *Biopolymers* 23 (1984) 1941–1961.
- [26] P.G. Wu, L. Song, J.B. Clendenning, B.S. Fujimoto, A.S. Benight, J.M. Schurr, Interaction of chloroquine with linear and supercoiled DNAs. Effect on the torsional dynamics, rigidity, and twist energy parameter, *Biochemistry* 27 (1988) 8128–8144.
- [27] M.J. Waring, Complex formation between ethidium bromide and nucleic acids, *J. Mol. Biol.* 13 (1965) 269–282.
- [28] J.B. LePecq, C. Paoletti, A fluorescent complex between ethidium bromide and nucleic acids. Physical–chemical characterization, *J. Mol. Biol.* 27 (1967) 87–106.
- [29] W. Mueller, D.M. Crothers, Interactions of heteroaromatic compounds with nucleic acids: 1. The influence of heteroatoms and polarizability on the base specificity of intercalating ligands, *Eur. J. Biochem.* 54 (1975) 267–277.
- [30] J.W. Nelson, I. Tinoco Jr., Intercalation of ethidium ion into DNA and RNA oligonucleotides, *Biopolymers* 23 (1984) 213–233.
- [31] M.W. Van Dyke, R.P. Hertzberg, P.B. Dervan, Map of distamycin, netropsin, and actinomycin binding sites on heterogeneous DNA: DNA cleavage-inhibition patterns with methidium-propyl-EDTA-Fe(II), *Proc. Natl. Acad. Sci. U. S. A.* 79 (1982) 5470–5474.
- [32] R.P. Hertzberg, P.B. Dervan, Cleavage of DNA with methidium-propyl-EDTA-iron(II): reaction conditions and product analyses, *Biochemistry* 23 (1984) 3934–3945.
- [33] B.S. Fujimoto, J.M. Schurr, Composition dependence of the torsional rigidity of DNA. Relevance to the affinity of 434 repressor for different operators, *Nature* 344 (1990) 175–178.
- [34] W.H. Press, S.A. Teukolsky, W.T. Vetterling, B.P. Flannery, *Numerical Recipes in Fortran 77*, Cambridge University Press, New York, 1999.
- [35] P.R. Bevington, *Data Reduction and Error Analysis for the Physical Sciences*, McGraw-Hill, New York, 1969.
- [36] P.J. Heath, J.B. Clendenning, B.S. Fujimoto, J.M. Schurr, Effect of bending strain on the torsion elastic constant of DNA, *J. Mol. Biol.* 260 (1996) 718–730.
- [37] J.D. Moroz, P. Nelson, Torsional directed walks, entropic elasticity, and DNA twist stiffness, *Proc. Natl. Acad. Sci. U. S. A.* 94 (1997) 14418–14422.
- [38] J.A. Gebe, S.A. Allison, J.B. Clendenning, J.M. Schurr, Monte Carlo simulations of supercoiling free energies for unknotted and trefoil knotted DNAs, *Biophys. J.* 68 (1995) 619–633.
- [39] J.A. Gebe, J.J. Delrow, P.J. Heath, D.W. Stewart, J.B. Clendenning, J.M. Schurr, Effects of  $\text{Na}^+$  and  $\text{Mg}^{2+}$  ions on the structures of supercoiled DNAs. Comparison of simulations with experiments, *J. Mol. Biol.* 262 (1996) 105–228.

- [40] J.J. Delrow, P.J. Heath, J.M. Schurr, On the origin of the temperature dependence of the supercoiling free energy, *Biophys. J.* 73 (1997) 2688–2701.
- [41] J.J. Delrow, P.J. Heath, B.S. Fujimoto, J.M. Schurr, Effect of temperature on DNA secondary structure in the absence and presence of 0.5 M tetramethylammonium chloride, *Biopolymers* 45 (1998) 503–515.
- [42] U.-S. Kim, B.S. Fujimoto, C.E. Furlong, J.A. Sundstrom, R. Humbert, D.C. Teller, J.M. Schurr, Dynamics and structures of DNA: long-range effects of a 16 base-pair sequence on secondary structure, *Biopolymers* 33 (1993) 1725–1745.
- [43] J.M. Schurr, J.J. Delrow, B.S. Fujimoto, A.S. Benight, The question of long-range allosteric transitions in DNA, *Biopolymers* 44 (1997) 283–308.
- [44] P.J. Hagerman, B.H. Zimm, Monte Carlo approach to the analysis of the rotational diffusion of wormlike chains, *Biopolymers* 20 (1981) 1481–1502.